ChemComm

Accepted Manuscript

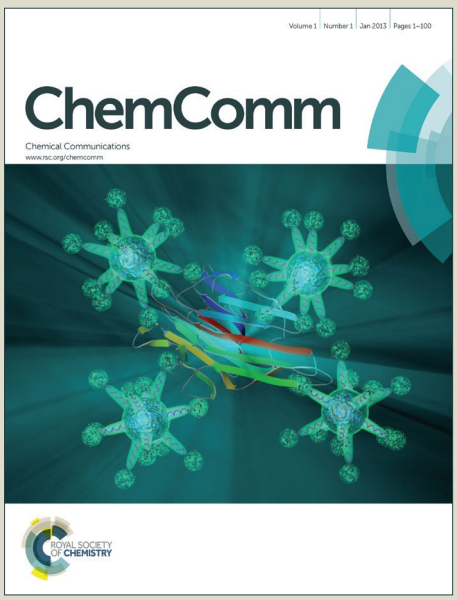

ROYAL SOCIETY OF CHEMISTRY

www.rsc.org/chemcomm

Cite this: DOI: 10.1039/c0xx00000x

www.rsc.org/xxxxxx

ARTICLE TYPE

Unusually High Thermal Stability and Peroxidase Activity of Cytochrome c in Ionic Liquids Colloidal Formulation

Pankaj Bharmoria,[a] Arvind Kumar[a,b*]

Received (in XXX, XXX) Xth XXXXXXXXX 20XX, Accepted Xth XXXXXXXXX 20XX
DOI: 10.1039/b000000x

Ionic liquid (IL) surfactant choline dioctylsulfosuccinate, [Cho][AOT] formed polydispersed vesicular structures in the IL, ethylmethylimidazolium ethylsulfate, [C_2mim][C_2OSO_3]. Cytochrome c dissolved in such a colloidal medium has shown very high peroxidase activity (~2 times to that in neat IL and ~4 times to that in aqueous buffer). Significantly, the enzyme retained both structural stability and functional activity in ILs colloidal solutions up to 180°C, demonstrating the suitability of system as high temperature bio-catalytic reactor.

Synthetic vesicular membranes have long been used as mimic to understand the phospholipid bio-membranes synergy with proteins.[1-3] Vesicles are colloidal bilayer architectures formed by surfactants upon aggregation beyond critical aggregation concentration.[4] In the living system, proteins-biomembrane synergy performs key functions like cell metabolism, signaling, cell gatekeeping and also act as drugs targets.[1] This synergy has been mimicked in vitro for commercial utility with synthetic surfactants as protein-surfactant colloidal formulations in pharmaceuticals, cosmetics, drug delivery, biochemical reactions and very recently in bioelectronics.[5] But most of these formulations are restricted to aqueous medium with in the range of room temperature.

The rise of ionic liquids (ILs, salts with melting points <100°C[6]) as thermally stable green solvents liaising with accessible solvating ability and surface activity has generated new opportunities to utilize them as a medium for the preservation of biomolecules and to develop thermally stable surfactant-protein colloidal formulations. However, there are several hurdles in the formulation of such colloidal systems in an IL medium because of (i) limited solubility of proteins[7] and surfactants, particularly the anionic surfactants,[8] (ii) high probability of structural alterations and functional deactivation of proteins,[9] and (iii) poor/weak self-assembly of surface active molecules. Despite these limitations, some of the ILs have been found suitable to dissolve proteins with a slightly perturbed structure with the retention of functional activity,[10] and support self-assembly of a variety of amphiphiles.[11] There are few reports of supramolecular assemblies such as "vesicles" of surfactants, lipids, or block copolymers in IL medium.[12] However, no report is yet available wherein both the protein and surfactant could be dissolved in a common IL, and therefore, the binding behavior of proteins with surfactants or surfactant like ILs in IL medium is completely unexplored.

Guided by the work of Malvika Bihari et al.[10] wherein Cytochrome c (Cyt c) could be homogeneously dissolved in [C_2mim][C_2OSO_3] with the retention of peroxidase activity at room temperature and our own previous work on the formation of vesicles and reverse vesicles of an IL surfactant in IL medium,[13] herein we report a novel colloidal formulation comprising of Cyt c- [Cho][AOT]-[C_2mim][C_2OSO_3] as constituents. Experimental details, materials, and dissolution characterics of Cyt c in [Cho][AOT]-[C_2mim][C_2OSO_3] are provided as Fig. S1-S5 (ESI†).

Initially we characterized the self-assembling behaviour of [Cho][AOT] in [C_2mim][C_2OSO_3] medium from the I_1/I_3 vibronic band ratio of pyrene as polarity probe, Fig. 1A and isothermal titration calorimetry (ITC), Fig. 1 B.

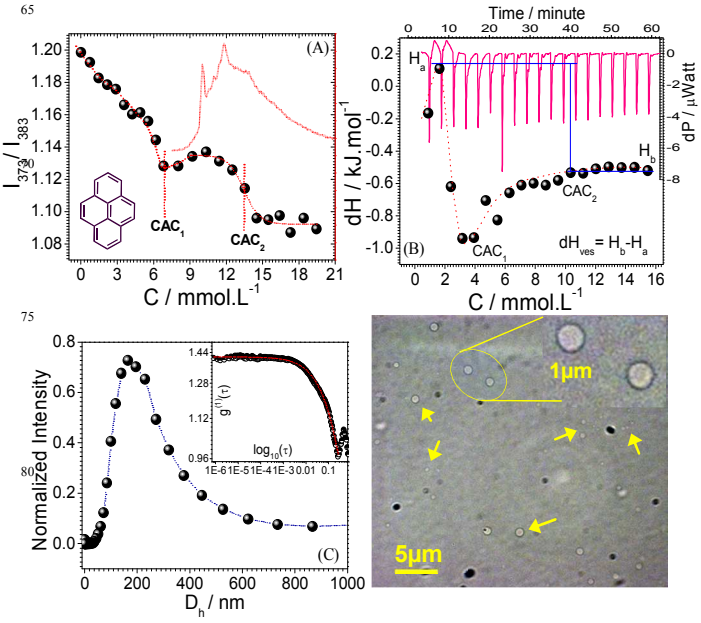

Fig. 1 (A) Pyrene I_1/I_3 vs [Cho][AOT] conc. curve along with fluorescence spectra of pyrene in [C_2mim][C_2OSO_3] shown as inset (B) Isothermal titration calorimetric plot of [Cho][AOT] dilution in [C_2mim][C_2OSO_3] with dP plot as inset. (C) D_h plot with corresponding autocorrelation function as inset, and (D) Optical images of [Cho][AOT] vesicles in [C_2mim][C_2OSO_3] medium (black spots in the figure are due to lens artefacts).

The I_1/I_3 ratio (1.20) of pyrene in the native $[C_2mim][C_2OSO_3]$ lies between highly non-polar and polar solvents and therefore, indicated the presence of various bicontinuous microphases, comprising of polar/non-polar domains.[14] Two transitions were observed in the Fig. 1A. The first transition at 5.5 mmol.L^{-1} (CAC_1) corresponds to the formation of pre-vesicular aggregates wherein some of the $[C_2mim][C_2OSO_3]$ molecules remain embedded in the aggregates of [Cho][AOT]. Above 5.5 mmol.L^{-1} the I_1/I_3 ratio increased a bit before decreasing in a sigmoidal fashion and became constant in the post-aggregation region. The constancy of I_1/I_3 ratio has indicated that pyrene senses uniform hydrophobic environment in the [Cho][AOT] aggregates. The second transition observed at 13.52 mmol.L^{-1}, corresponds to critical vesicular concentration (CAC_2). Such an aggregation behavior has been previously observed for CTAB in $C_6mim]Br/H_2O$ and $[C_4mim]Br/H_2O$ mixtures.[15]

The ITC curve (Fig. 1B) also confirmed the aggregation of [Cho][AOT] in $[C_2mim][C_2OSO_3]$ medium. The negative enthalpy changes observed from the enthalpogram indicates that in the aggregation process of [Cho][AOT], van der Waal's interactions are dominating over electrostatic interactions between [Cho][AOT] and $[C_2mim][C_2OSO_3]$.[13] It is to be noted that Gordon parameter (G), an indicator of the solvophobic effect of a solvent to support self-assembly is 0.846 for $[C_2mim][C_2OSO_3]$[11a] and is higher than 0.463 of $[C_4mim]$ $[Tf_2N]$ reported earlier to support self-assembly of $[ProC_3][LS]$.[13] Therefore, the good solvophobicity of $[C_2mim][C_2OSO_3]$ can be accounted as one of the reason to support the self-assembly of [Cho][AOT]. The Gibbs free energy of aggregation, ΔG^o_{agg}, (-14.4 kJ.mol^{-1}) was calculated using the mass action model (Annexure 1 ESI†) by considering the ionization degree of aggregation (α) as 1 due to the exclusively ionic shell surrounding the aggregates in IL medium. Negative value of ΔG^o_{agg} has indicated the feasibility of [Cho][AOT] self-assembly in $[C_2mim][C_2OSO_3]$. The entropic contribution ($T\Delta S^o_{agg}$) to the ΔG^o_{agg} was determined from standard Gibbs free energy equation (Annexure 1 ESI†) and was found to be 14.82 kJ.mol^{-1}. The high $T\Delta S^o_{agg}$ value compared to ΔH^o_{agg} (-0.42 kJ.mol^{-1}) has indicated that the aggregation process is mainly entropy driven.

The formation of aggregated structures was confirmed from DLS measurements (Fig. 1C). The hydrodynamic diameter (D_h) of [Cho][AOT] (50 mmol.L^{-1}) aggregates in $[C_2mim][C_2OSO_3]$ medium at an scattering angle of 90^o and 298.15 K was found to be 164 nm which is comparable to that of [Cho][AOT] vesicles in water (150 nm).[16] Upon comparing the intensity autocorrelation function of the scattered light by [Cho][AOT] aggregates in $[C_2mim][C_2OSO_3]$ and aqueous medium (Fig. S6 ESI†) it was found that the decay time (τ) in $[C_2mim][C_2OSO_3]$ (τ =1.63 ms) is two order of magnitude higher than that in water (τ =17.6 µs). Slow relaxation of scattered light in $[C_2mim][C_2OSO_3]$ can possibly be accounted to its high viscosity (97.58 cP compared to 0.890 cP that of water at 25^{o}C).[17] In sight of more transparent understanding of the in situ aggregate size, we performed multi-angles DLS measurements from 30^o to 150^o (Fig. S7 ESI†). The hydrodynamic diameter D_h increased from 130 nm to 600 nm as the angle varied from 30^o to 150^o, thus indicating the polydispersed nature of aggregates. In order to reveal the morphology of [Cho][AOT] aggregates in $[C_2mim][C_2OSO_3]$ medium we performed optical microscopy (Fig. 1D, Fig. S8, ESI†). The microscopic images showed spherical droplets in the size range of 0.1 to 1 µm. The droplets observed are the polydispersed vesicles. Similar observation of formation of vesicles of an IL in IL medium has been reported by us in our previous communication (*Chem Commun.* 2013)[13]. [Cho][AOT] self-assemblies in $[C_2mim][C_2OSO_3]$ were found to be kinetically stable at room temperature as no precipitation or phase separation was observed for 10 months even at a concentration as high as 300 mmol.L^{-1}. The proposed structure of [Cho][AOT] vesicles in $[C_2mim][C_2OSO_3]$ medium is depicted in Fig. S9 (ESI†).

We explored the application of [Cho][AOT]- $[C_2mim][C_2OSO_3]$ colloidal system as high temperature preservative for the enzyme Cyt c by investigating its binding behavior, conformational stability and functional activity. The binding isotherm of [Cho][AOT] to Cyt c (15 µM) dissolved in $[C_2mim][C_2OSO_3]$ (Fig. 2A) has been defined by subtracting the dilution enthalpogram of [Cho][AOT] in $[C_2mim][C_2OSO_3]$ medium from that of Cyt c-$[C_2mim][C_2OSO_3]$ solution (Fig. S10). In surfactant-protein systems the surfactant interacts with protein in different forms (monomers at low concentration, protein induced aggregates in the mid concentration region and micelle or vesicles, post CAC).[18] The binding of [Cho][AOT] to Cyt c at low concentration is an endothermic process whereas the binding of [Cho][AOT], aggregates and vesicles to Cytochrome is an exothermic process with a small change in enthalpy. It is to be noted that small enthalpy changes upon binding to proteins occurs when interactions are electrostatic in nature.[19] Therefore, the small enthalpy changes indicates that [Cho][AOT] binds to Cyt c mainly through electrostatic interactions.[19]

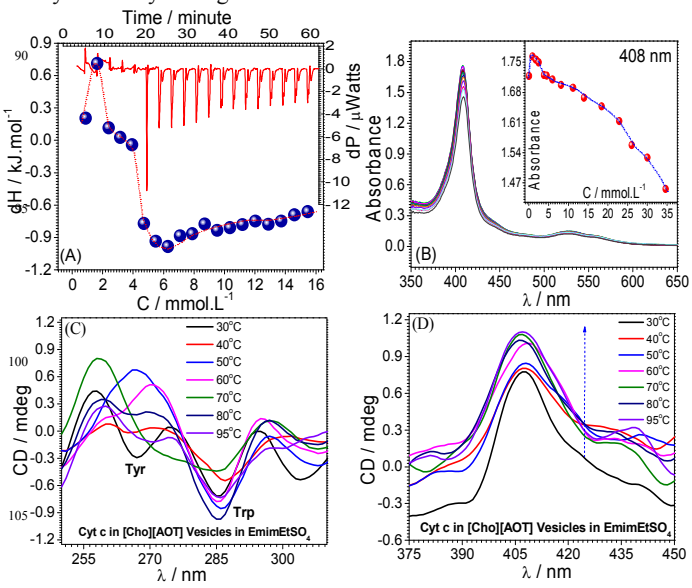

Fig. 2 (A) Binding isotherm of [Cho][AOT] binding to Cyt c (15 µM) in neat $[C_2mim][C_2OSO_3]$; (B) UV-Vis spectra of Cyt c (15 µM) in at different [Cho][AOT] concentrations; (C, D) Mid-UV CD spectra of Cyt c in [Cho][AOT] (100mM)+ $[C_2mim][C_2OSO_3]$.

Alterations in structure of Cyt c upon [Cho][AOT] binding at different concentrations were measured from the changes in UV-Vis spectra (Fig. 2B). In the neat $[C_2mim][C_2OSO_3]$, Cyt c showed an intense soret band at 408 nm and weak Q bands at 528 and 556 nm due to π-π* transition in the heme group buried deep inside the hydrophobic core of protein.[10a] Upon addition of [Cho][AOT] a slight increase in absorbance of Cyt c was observed in the low concentration followed by a continuous decrease in absorbance at higher concentrations. The decrease in absorbance (hypsochromic shift) occurs due to the lowering in energy of π* orbital upon exposure to the surrounding polar environment which is possible due to the unfolding of protein around the heme cleft. Though an unfolding was observed around the heme cleft, unlike the aqueous formulation, the oxidation state of Cyt c did not change at any concentration as indicated by

the retention of Q bands at 528 and 556 nm. Due to the absorption of imidazolium in the far UV-region we could not observe the secondary structure of Cyt c from CD-measurements. But when we compared the mid-UV CD spectra, the bands due to Tyr and Trp were observed at 263 and 287 nm but Phe band was missing (Fig. S11, ESI†). Therefore, compared to water the Tyr and Trp residues experienced more nonpolar environment which can be due to the presence various non-polar domains in $[C_2mim][C_2OSO_3]$.[14] Upon addition of 100 mM [Cho][AOT] a bathochromic shift of 4 nm in the band at 263 nm and a hypsochromic shift of 2 nm in the band at 287 was observed which indicated that conformation of protein in vesicles is such that Trp which is present around the heme pocket faces the hydrophobic tail part of vesicle. The rise in ellipsity (θ) of Tyr and Trp residue indicated the stabilization of the tertiary structure of protein.

We also checked the thermal stability of the Cyt c in the vesicular regime by measuring the temperature dependent CD spectra of Tyr and Trp residues (Fig.2C) and soret band at 408 nm (Fig.2D). The band due to Tyr at 267 nm disappeared with the rise in temperature which indicated conformational changes in the protein backbone as three of the Tyr residues are usually present in the protein backbone. The overall θ of bands (at 286 nm due to Trp and soret band at 408 nm) increased with respective signs upon increasing the temperature from 30 to 95°C without deformation of the CD bands which indicated the thermal stability of proteins tertiary structure in the region around heme cleft. Because of inbuilt temperature limitations of CD and UV-Vis spectrophotometers, the measurements above 100°C were carried out by heating the samples outside the spectrophotometer using a silicon oil bath. The CD and UV-Vis spectra of incubated samples were then recorded. Comparative CD and UV-Vis spectra of Cyt c dissolved in $[C_2mim][C_2OSO_3]$ and [Cho][AOT]-$[C_2mim][C_2OSO_3]$ measured at different temperatures and time periods are provided in Fig. S12 and Fig. S13 (ESI†). Retention of CD soret at 408 nm and UV soret and Q bands indicated the structural stabilization of Cyt c around the heme cleft. It has been observed that Cyt c remains stable up to 180°C for a maximum of 5 min. whereas at 130°C it remains stable for a time period 1 h. These conclusions were arrived at by checking the structural stabilization of Cyt c for more than 1 h at 130°C and for 1h at 140°C, wherein the Cyt c was found to lose its activity. It has also been observed that the time period for structural stabilization of Cyt c increased with the decrease in temperature as evident from its spectra at 100°C after 6 h of heating (Fig. S12A, B and S13A). Comparison of the stabilization of Cyt c in $[C_2mim][C_2OSO_3]$ and [Cho][AOT]-$[C_2mim][C_2OSO_3]$ solutions showed that Cyt c remains more stable in later which is evident from the higher ellipsity of CD soret band at 408 nm (Fig. S12) and higher absorbance of UV soret and Q bands (Fig. S13). Therefore, the [Cho][AOT] vesicles imparted extra thermal stability to Cyt c in the colloidal formulation.

The activity of Cyt c (30 μM) in $[C_2mim][C_2OSO_3]$ or [Cho][AOT]-$[C_2mim][C_2OSO_3]$ was investigated by incubating the Cyt c solutions for 10 min in the temperature range of 60 to 180°C. After incubation the catalytic activity was observed using guaiacol as substrate and H_2O_2 as an oxygen donor at room temperature. Cyt c catalyses the oxidation of guaiacol to tetraguaiacol which gives orange colour and show absorption band at 470 nm (Fig. S14 and S15, ESI†).[20] Qualitatively the activity was monitored by visual inspection of the appearance of orange colour (Fig. 3).

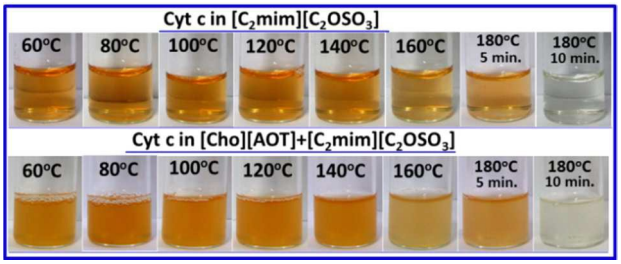

Fig. 3 Functional activity of Cyt c in $[C_2mim][C_2OSO_3]$ and [Cho][AOT](100mM)-$[C_2mim][C_2OSO_3]$ from 60 to 180°C.

Cyt c retained its functional activity up to 180°C for maximum 5 min and 160°C for maximum 10 min both in neat $[C_2mim][C_2OSO_3]$ and [Cho][AOT]-$[C_2mim][C_2OSO_3]$ vesicular solution. 180°C is considered as highest activity temperature on account of the fact that maximum product formation occurs within five minutes of the reaction inception (Fig. S16, ESI†). Quantitatively the tetraguaiacol formation was calculated from the absorption changes at 470 nm and molar extinction coefficient of 2.66×10^4 $cm^{-1}.M^{-1}$ (Fig. S17, ESI†). The activity of Cyt c in the [Cho][AOT]-$[C_2mim][C_2OSO_3]$ vesicular solutions was found to be ~2 fold higher than that observed in neat $[C_2mim][C_2OSO_3]$ at all the temperatures (Fig.4A).

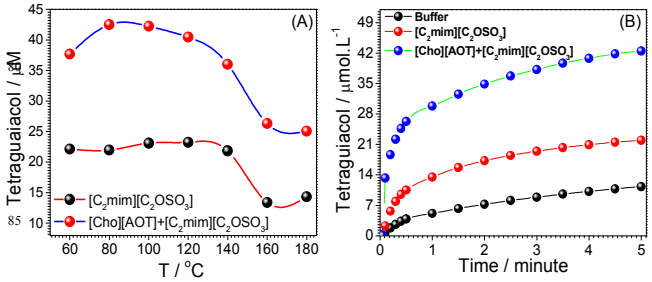

Fig.4. (A) Temperature dependent activity of Cyt c (30 μM) in neat $[C_2mim][C_2OSO_3]$ and [Cho][AOT] (100mM) + [-$[C_2mim][C_2OSO_3]$ solutions; (B) activity of Cyt c in buffer, neat $[C_2mim][C_2OSO_3]$ and [Cho][AOT](100mM)+$[C_2mim][C_2OSO_3]$ vesicular solutions after incubation at 80°C

The higher activity in vesicular solution can be attributed to (i) exposure of the catalytic iron centre of enzyme due to slight perturbation in conformation around the heme cleft[10a] as observed from the UV-Vis and CD spectra (Fig. 2B, C and D), (ii) higher thermal stability imparted by [Cho][AOT] vesicles in [Cho][AOT]-$[C_2mim][C_2OSO_3]$ system (Fig. S12 and S13, ESI†). Since Cyt c retained its activity in buffer solution till 80°C, we did a comparative analysis of the activity of Cyt c in buffer, neat $[C_2mim][C_2OSO_3]$ and [Cho][AOT] (100 mM)-$[C_2mim][C_2OSO_3]$ vesicular solutions by incubating the enzyme at 80°C (Fig. 4B). It has been found that the activity of Cyt c in [Cho][AOT]-$[C_2mim][C_2OSO_3]$ vesicular solution after 5 min of incubation is ~4 fold higher than in buffer and ~2 fold higher than in neat $[C_2mim][C_2OSO_3]$. The initial rates of enzymatic reactions were calculated from the maxima of the first derivatives of product formation curve ($r = d(P)/dt$). Due to the technical limitation of UV-Vis instrument to detect the absorbance changes below 0.5 min we extrapolated the product formation curve to

zero value in order to calculate the initial rate of reaction. It has been found that the initial rate of enzymatic reaction in [Cho][AOT]-[C_2mim][C_2OSO_3] solutions (158.8 μM.min.$^{-1}$) is 4 fold higher than that in neat [C_2mim][C_2OSO_3] (39.2 μM.min.$^{-1}$) and 13 fold higher than in buffer (12.17 μM.min.$^{-1}$). High activity of Cyt c has earlier been reported in ILs ([C_4mim][Tf_2N], [C_4mim][PF_6] and [C_8mim][PF_6]) solutions of methanol/crown ether at 40^{o}C with the addition of pyridine.[21] The higher activity of Cyt c herein can also be accounted to the more collision of substrate and exposed catalytic iron centre of Cyt c. Vesicles provide suitable water-vesicle interface with large interfacial area to increase the contacts between substrate and enzyme active sites similar to that observed for micellar catalysis by enzymes in ILs.[22] The redox activity of Cyt c was also analysed at maximum temperature (130^{o}C) of stabilization for 1h and at 100^{o}C for 6 h, wherein Cyt c was found to be redox active (Fig. S18). Such a redox activity has previously been reported by Tamura et al. in IL, [Amim][Cl] in the temperature range of 120 to 140^{o}C for 3 h using optical-waveguide (OWG) spectroscopy. Authors cited the importance of polar ILs with hydrogen bond basicity, β>0.7 as one of the reason for protein solubilization and stabilization.[23] The β of [C_2mim][C_2OSO_3] is 0.71 and therefore must be one of the reasons for Cyt c solubilisation and stabilization. Further, the decrease in stabilization time with temperature can be accounted to the thermal stability of [C_2mim][C_2OSO_3] with a flash point of 162^{o}C, thereafter slow degradation of [C_2OSO_3] anion begins to happen[24] thus introducing the volume effects towards structural and functional stability.

Conclusions

It has been shown that [C_2mim][C_2OSO_3] is a unique IL which can dissolve the enzyme Cyt c with slight conformational alterations and can also support the self-assembly of anionic surface active IL [Cho][AOT] in the form of vesicles. The hydrogen bond basicity, β=0.71 and good solvophobicity (G= 0.846) of [C_2mim][C_2OSO_3] can be accounted as reasons of Cyt c solubility and [Cho][AOT] self-assembly in [C_2mim][C_2OSO_3]. Cyt c thus dissolved in [Cho][AOT]-[C_2mim][C_2OSO_3] vesicular solutions retained its functional activity up to very high temperatures for different time periods. The results demonstrate the potential of ILs colloidal solutions as media for preservation of enzymes, and as enzymatic catalytic reactors at elevated temperatures.

Financial support from DST, India for this work (No. SB/S1/PC-104/2012) is acknowledged. We thank the Centralized Instrumental Facility, Mr. Sant Lal, Praveen Singh Gehlot and Damarla Krishniah for assistance in various capacities.

Notes and references

[a]*AcSIR, CSIR-Central Salt and Marine Chemicals Research Institute.*
[b]*Salt and Marine Chemicals Division, CSIR-Central Salt and Marine Chemicals Research Institute, Bhavnagar-364002, India. Fax: +91-278-2567562.; Tel: +91-278-2567039; E-mail: arvind@csmcri.org*

†Electronic Supplementary Information (ESI) available: Materials, methods, purity specifications (Table S1) and experimental details (Fig. S1-S5), equations used are given as annexure-I, Detailed results are given as supporting information. See DOI: 10.1039/b000000x/

1. U. H. N. Dürr, M. Gildenberg, A. Ramamoorthy, *Chem. Rev.* 2012, **112**, 6054-6074.
2. M. N. Jones, *Chem. Soc. Rev.* 1992, **21**, 127-136.
3. E. Soussan, S. Cassel, M. Blanzat, I. Rico-Lattes, *Angew. Chem., Int. Ed.* 2009, **48**, 274-288.
4. J. N. Israelachvili, Intermolecular and Surface Forces, Academic Press, New York, 1992.
5. K. P. Ananthapadmanabhan, E. D. Goddard, In Interactions of Surfactants with Polymers and Proteins. CRC Press, Inc: London, U.K., **1993**; Chapter 8.
6. Green Industrial Applications of Ionic Liquids, ed. R. D. Rogers, K. R. Seddon and S. Volkov, NATO Science Series, Kluwer, Dordrecht, 2002.
7. Lau, R. M.; Sorgedrager, M. J.; Carrea, G.; van Rantwijk, F.; Secundo, F.; Sheldon, R. A. Green Chem. 2004, **6** , 483–487.
8. M. Moniruzzaman, N. Kamiya, K. Nakashima, M. Goto, *Chem Phys Chem*, 2008, **9**, 689–692.
9. Vrikkis, R. M.; Fraser, K. J.; Fujita, K.; MacFarlane, D. R.; Elliott, G. D. J. Biomech. Eng.-Trans. ASME 2009, 131 XXX.
10. M. Bihari, T. P. Russell, D. A. Hoagland, *Biomacromolecules*, 2010, **11**, 2944-2978; N. Byrne, L. M. Wang, J. P. Belieres, C. A. Angell, *Chem. Commun.* 2007, **26**, 2714–2716; D. Constatinescu, C. Herrmann, H. Weingartner, *Phys. Chem. Chem. Phys.* 2010, **12**, 1756-1763; J. P. Mann, A. McCluskey, R. Atkin, *Green Chem.* 2009, **11**, 785–792; Byrne, N.; Belieres, J. P.; Angell, C. A. *Aust. J. Chem.* 2009, **62**, 328-333; K. Tamura, N. Nakamura, H. Ohno, *Biotechnol. Bioeng*. 2012, **109**, 729–735.
11. T. L. Greaves, C. J. Drummond, *Chem. Soc. Rev.* 2013, **42**, 1096-1120; B. Fernández-Castro, T. Méndez-Morales, J. Carrete, E. Fazer, O. Cabeza, J. R. Rodríguez, M. Turmine, L. M. Varela, *J. Phys. Chem. B* 2011, **115**, 8145–8154; L. Shi, L. Zheng, *J. Phys. Chem. B* 2012, **116**, 2162-2172.
12. T. Nakashima, N. Kimizuka, *Chemistry Letters*, 2002, 1018-1019; J. Hao, A. Song, J. Wang, X. Chen, W. Zhuang, F. Shi, F. Zhou, W. Liu, *Chem. Eur. J.* 2005, **11**, 3936-3940; C. R. López-Barrón, D. Li, L. DeRita, M. G. Basavaraj, N. J. Wagner, *J. Am. Chem. Soc.* 2012, **134**, 20728-20732; F. Gayet, J.-D. Marty, A. Brûlet, N. Lauth-de Viguerie, *Langmuir* 2011, **27**, 9706-9710; Z. Bai, T. P. Lodge, *J. Am. Chem. Soc.* 2010, **132**, 16265–16270; R. R. Maddikeri, S. Colak, S. P. Gido, G. N. Tew, *Biomacromolecules* 2011, **12**, 3412-3417.
13. K. S. Rao, S. Soo; A. Kumar, *Chem Commun*. 2013, **49**, 8111-8113.
14. J. N. C. Lopes, A. A. H. Pádua, *J. Phys. Chem. B* 2006**, 110***,* 3330-3335; T. S. Kang, K. Ishiba, M. Morikawa, N. Kimizuka, *Langmuir*, 2014, **30**, 2376-2384.
15. S. Javadian, V. Ruhi, A. Heydari, A. A. Shahir, A. Yousefi, J. Akbari, *Ind. Eng. Chem. Res*. 2013, **52**, 4517-4526.
16. P. Bharmoria, T. J. Trivedi, A. Pabbathi, A. Samanta, A.Kumar, *Phys. Chem. Chem. Phys.* 2015, **17**, 10189-10199.
17. E. Gómez, B. González, N. Calvar, E. Tojo, Á. Domínguez, *J. Chem. Eng. Data* 2006, **51**, 2096-2102.
18. D. Otzen, *Biochim. Biophys. Acta* 2011, **1814**, 562-591.
19. P. D. Ross, S. Subramanian, *Biochemistry*, 1981, **20** 3097-3102.
20. R. E. M. Diederix, M. Ubbink, G. W. Canters, *Eur. J. Biochem*. 2001, **268**, 4207-4216.
21. J. A. Laszlo, D. L. Compton, *J Mol. Cat. B: Enz.* 2002, **18**, 109-120.
22. S. P. M. Ventura, L. D. F. Santos, J. A. Saraivab, J. A. P. Coutinho, *Green Chem.*, 2012, **14**, 1620-1625; H. Stamatis, A. Xenakis and F. N. Kolisis, *Biotechnol. Adv.*, 1999, **17**, 293-318; A. Shome, S. Roy and P. K. Das, *Langmuir*, 2007, **23**, 4130-4136.
23. K. Tamura, N. Nakamura, H. Ohno, *Biotech. Bioeng.* 2012, **109**, 729-735.
24. A. Fernández, J. S. Torrecilla, J. García, F. Rodríguez, *J. Chem. Eng. Data* 2007, **52**, 1979-1983.

